Modeling and Comparison of Fuzzy-PI and Genetic Control Algorithms for Active and Reactive Power Flow between the Stator (DFIG) and the Grid

Abdelhafid Guediri
University of El Oued, VTRS Laboratory, Faculty of Technology, El Oued, Algeria
abdelhafid-guediri@univ-eloued.dz

Abdelkarim Guediri
University of El Oued, VTRS Laboratory, Faculty of Technology, El Oued, Algeria
karim_elect@yahoo.fr

Slimane Touil
University of El Oued, VTRS Laboratory, Faculty of Technology, El Oued, Algeria
slimanetouil@yahoo.fr

Received: 11 March 2022 | Revised: 27 March 2022 and 31 March 2022 | Accepted: 4 April 2022

Abstract-This paper performs a comparison between Fuzzy-PI regulators and Genetic Algorithm (GA) for controlling an active and reactive Doubly-Fed Induction Generator (DFIG) for providing power to the electrical grid. Theoretical analysis, modeling, and simulation studies are provided. Control strategies were developed for both active and reactive forces in order to optimize energy production. The performance of the two control strategies was examined and compared using benchmarks for durability and reference traceability. This paper studied a system consisting of a wind turbine operating at variable wind speed and a two-feed asynchronous machine (DFIG) connected to the grid by the stator and fed by a transducer at the side of the rotor. The conductors were separately controlled for active and reactive power flow between the stator (DFIG) and the grid, which was achieved in this article using conventional PI and fuzzy logic controllers. The considered controllers generated reference voltages for the rotor to ensure that the active and reactive power reached the required reference values. This was done in order to ensure effective tracking of the optimum operating point and the maximum output of electrical power. System modeling and simulation were examined in Matlab/Simulink. Dynamic analysis of the system was performed under variable wind speed.

Keywords-Genetic Algorithm (GA); fuzzy logic controller (FC); Doubly Fed Induction Generator (DFIG); variable speed wind turbine; conventional PI controller; Maximum Power Point Tracking (MPPT)

I. INTRODUCTION

Globally, wind power has become the fastest growing renewable energy source. Wind turbine speed control is generally used to improve energy production. DFIG-based wind power transmission systems offer various advantages, including reducing stress on mechanical structures and acoustic noise with the ability to control active and reactive energy. Another feature of the DFIG system is that the connected AC/DC/AC PWM transformers between the grid and the rotating circuit of the induction generator are designed for only a portion of the generator power [1]. Wind power generation implementation was introduced on the basis of DFIG, a fuzzy PI gain scheduling developed for DFIG vector control units used in variable speed wind turbines [2]. Upon theoretical analysis of the wind turbine and DFIG processing, due to mathematical models of the system, a DFIG separation control was developed based on a fuzzy-PI controller in [3]. Wind power generation by DFIG can be connected directly to the grid via the stator, which is driven by a direct AC/DC inverter. The relative complexities (in size or structure) of the research space and the function to be improved lead to the use of radically different precision methods [4].

While the stochastic methods are the more efficient and effective, they use processes based on stochastic exploration of the space of possible solutions [5]. Among the latter, we find Genetic Algorithms (GAs) that represent a rich and interesting family of stochastic optimization algorithms. They are inspired by concepts of evolution and natural selection and the probabilistic research based on the mechanism of natural selection and genetics. GAs are highly effective and robust in a general set of problems. GAs maintain a set of encoded solutions and this group is geared towards the optimal solution [6]. In order to find an ideal solution to a problem in a complex space, it is necessary to find a compromise between two goals: to explore better solutions and to aggressively exploit the search space. Analytical studies have shown that GAs manage this trade-off optimally [7].

II. DFIG MODEL WITH STATOR FLUX ORIENTATION

The orientation of the voltage and the stator flux is shown in Figure 1.

The DFIG electrical state can be modeled using the Park transform, as follows [8]:

Corresponding author: Abdelhafid Guediri

$$\begin{cases} V_{sd} = R_s I_{sd} + \frac{d\varphi_{sd}}{dt} \\ V_{sq} = R_s I_{sq} + \omega_s \varphi_{sd} \\ V_{rd} = R_r I_{rd} + \frac{d\varphi_{rd}}{dt} - (\omega_s - \omega)\varphi_{rq} \\ V_{rq} = R_r I_{rq} + \frac{d\varphi_{rq}}{dt} + (\omega_s - \omega)\varphi_{rd} \end{cases} \quad (1)$$

$$\begin{cases} \varphi_{sd} = L_s I_{sd} + M I_{rd} = \varphi_s \\ \varphi_{sq} = L_s I_{sq} + M I_{rq} = 0 \\ \varphi_{rd} = L_r I_{rd} + M I_{sd} \\ \varphi_{rq} = L_r I_{rq} + M I_{sq} \end{cases} \quad (2)$$

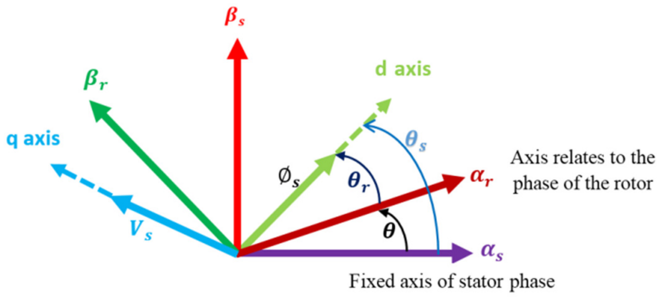

Fig. 1. Direction of stator voltage and flux.

To obtain separate control over the stator reactive and active forces, the DFIG model is required to express all quantities. This is in accordance with the concept of stator flow direction and assumes that the stator resistance is small compared to the stator reactance of a DFIG of medium and high power volume, where the stator flux can be computed as [9]:

$$\begin{cases} V_{sd} = \frac{d\varphi_{sd}}{dt} = 0 \\ V_{sq} = \omega_s \varphi_{sd} = V_S \end{cases} \quad (3)$$

$$\varphi_S = \frac{V_S}{\omega_S} \quad (4)$$

From the system of equations (2), we obtain:

$$\begin{cases} I_{sd} = \frac{\varphi_S}{L_s} - \frac{M}{L_s} I_{rd} \\ I_{sq} = -\frac{M}{L_s} I_{rq} \end{cases} \quad (5)$$

The stator reactive forces for DFIG are:

$$\begin{cases} P_s = V_{sq} I_{sq} \\ Q_s = V_{sq} I_{sd} \end{cases} \quad (6)$$

$$\begin{cases} P_s = -V_s \frac{M}{L_s} I_{rq} \\ Q_s = \frac{V_s \varphi_s}{L_s} - \frac{V_s M}{L_s} I_{rd} \end{cases} \quad (7)$$

The electromagnetic torque is expressed as:

$$C_{em} = -p \frac{M}{L_s} \varphi_s I_{rq} \quad (8)$$

The relationship of rotor voltage is given as:

$$\begin{cases} V_{rd} = R_r I_{rd} - g\omega_s (L_r - \frac{M^2}{L_s}) I_{rq} \\ V_{rq} = R_r I_{rq} + g\omega_s (L_r - \frac{M^2}{L_s}) I_{rd} + g\omega_s \frac{M\varphi_s}{L_s} \end{cases} \quad (9)$$

III. INDIRECT CLOSED LOOP FUZZY CONTROL

In this method, decoupling is performed at the level of the outputs of the rotor current regulators with system feedback. This allows the regulation of powers. One thus distinguishes a control by a loop in a cascade of the power and the rotor current for each axis, since this makes possible to separately control the currents I_{rd} and I_{rq} and the powers Q_s and P_s in a closed loop [10]. According to the reference torque delivered by the Maximum Power Point Tracking (MPPT) control, the rotor side converter guarantees a decoupled active and reactive stator power control, P_s and Q_s (MPPT). By holding the DC bus at a steady voltage level and imposing the reactive power Q_L at zero, the grid side converter controls the power flow exchange with the grid through the rotor [11]. The simplified diagram of this control assembly is illustrated in Figure 2.

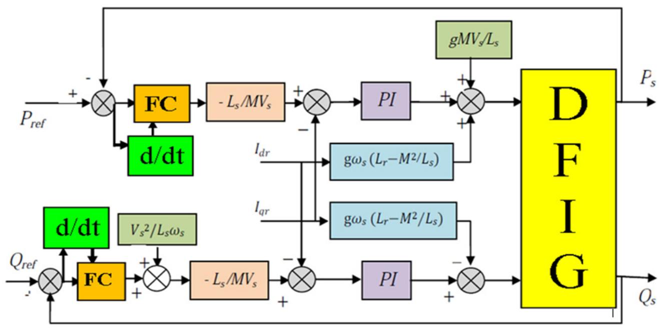

Fig. 2. Indirect closed loop fuzzy control diagram.

IV. FUZZY INFERENCE RULES

The rules of inference can be described in several ways, either linguistically, symbolically or by inference matrix. In the latter case, a so-called inference matrix brings together all the inference rules in the form of a table. In the case of a two dimensional array, the array entries represent fuzzy sets of the input variables [12].

TABLE I. RULE TABLE OF THE FUZZY CONTROLLER

ΔU		E						
		NG	NM	NP	EZ	PP	PM	PG
Δe	NG	NG	NG	NG	NM	NP	NP	EZ
	NM	NG	NM	NM	NM	NP	EZ	PP
	NP	NG	NM	NP	NP	EZ	PP	PM
	EZ	NG	NM	NP	EZ	PP	PM	PG
	PP	NM	NP	EZ	PP	PP	PM	PG
	PM	NP	EZ	PP	PM	PM	PM	PG
	PG	EZ	PP	PP	PM	PG	PG	PG

The linguistic variables are noted as follows: NG for large negative, NP for small negative, EZ for approximately zero, PP for small positive, PG for large positive, NM for mean negative, and PM for mean positive. E is the error, Δe is the error variation, and ΔU the controller output. The table gives forty-nine rules. For example:

R1 : IF E = NG AND Δe = NG THEN ΔU = NG.

V. DESCRIPTION AND DEVELOPMENT OF THE FUZZY CONTROLLER

Our goal is to control the rotor currents of a dual-power DFIG. The developed controller uses the scheme proposed by [13]. This diagram is represented by Figure 3. The output of the regulator is given by:

$$V_{rd}^{v} = V_{rd}^{v}(k-1) + du(k) \quad (10)$$

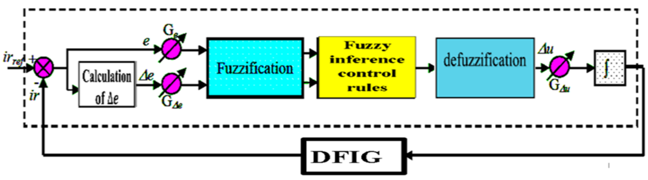

Fig. 3. Block diagram of the fuzzy controller.

The considered uses of the fuzzy controller include [14]:

- The triangular and trapezoidal membership functions. This choice is done due to the simplicity of implementation.
- A universe of standardized discourses.
- The universe of discourses is divided into seven fuzzy sets (fine tuning) for the input and output variables. A very fine subdivision of this universe on more than seven fuzzy sets does not generally bring any improvement in the dynamic behavior of the system to be regulated.
- Mamdani's [13] implication for inference.
- The center of gravity method for defuzzification.

For every gene that mutates, we take numbers τ and r. The first can take the values +1 for an effective alternate and -1 for a negative trade. The second is a randomly generated range within the variety (0 1). It determines the value of the trade. Under those conditions, the C_i' gene, which replaces the mutated gene, is calculated from one of the following relationships [15]:

$$\begin{cases} C_i' = C_i + (C_{max} - C_i)\left(1 - r^{\left(1-\frac{G_F}{G_T}\right)^5}\right) & \text{if } \tau = +1 \\ C_i' = C_i - (C_i - C_{min})\left(1 - r^{\left(1-\frac{G_F}{G_T}\right)^5}\right) & \text{if } \tau = -1 \end{cases} \quad (11)$$

where C_{max} and C_{min} denote, respectively, the lower and higher limits of the price of the parameter C_i, and GF≤GT represents the era for which the amplitude of the mutation cancels out.

The procedure for optimizing the parameters of the regulators can be summarized by the following steps [16]:

- Randomly generate an initial population.
- Evaluate this population.
- Apply genetic operators (selection, crossing, mutation).
- Evaluate the new population created by the genetic operators.

In the following, we will apply this procedure to the two regulators, classical PI and fuzzy PI. Hybridization method: simplex. The complete control diagram is shown in Figure 5.

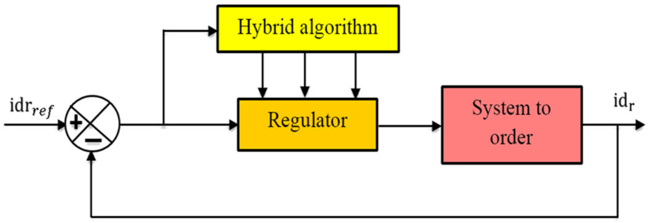

Fig. 4. Principle of optimization by genetic gradient or simplex algorithm.

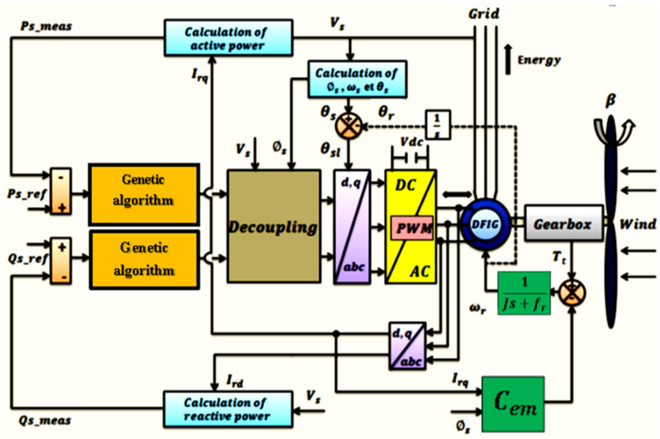

Fig. 5. Global block diagram of the command of the GA based on DFIG.

VI. COMPARISON OF THE CLASSIC GA AND FUZZY-PI REGULATOR

Fuzzy logic or fuzzy set theory has attracted the attention of a large number of researchers. Fuzzy logic control is regarded higher than the GA because it does not require precise mathematical models of the system [17]. Its strength and simplicity are the primary reasons for its use. In this work, we will develop a blur controller. The feasibility and performance of this controller have been verified in simulations of the control element that controls the exchange of active and reactive powers generated by an asynchronous machine with a dual power supply connected to a medium voltage network by acting on rotor signals via a bidirectional converter. The obtained numerical simulation results prove the growing interest in such control of electrical systems [18]. Tuning by fuzzy logic may override tuning by PI with respect to the quality of the dynamic response of the system. Indeed, the latter further reduces the response time by producing a limited overshoot accompanied by weak oscillations around the setpoint. In steady state, the precision is not as good as that of a PI regulator, where the integral action eliminates the static error; this then suggests the combination of the two types of regulators:

- A fuzzy regulator for the transient regime and
- a PI regulator for the steady state.

The major drawback of fuzzy regulators is the matching of gains, ensuring system stability. In addition, the order is calculated only from two values: the error and its variation [19].

VII. SIMULATION RESULTS

The results of the wind energy system simulation (turbine + DFIG) are controlled by fuzzy logic and GA. This paper displays the results of the different curves obtained by controlling the energetic and reactive forces generated at the stator level of the DFIG. This allows separating the expressions of the active and reactive powers of the generator or bears those of the flow and torque. The system first starts up without load. Then, an active reference force is applied:

Active power:

- Between t = 0s and t =0.2s (P_{ref} = 0 VAR).
- Between t = 0.2s and t = 0.6s negative scale (P_{ref} = -5000W).
- Between t = 0.6s and t = 1s (P_{ref} = 0W).

Reactive power:

- Between t = 0s and t =0.2s (Q_{ref} = 0 VAR).
- Between t = 0.2s and t = 0.6s negative scale (Q_{ref} = -5000 VAR).
- Between t = 0.6s and t = 1s (Q_{ref} = 0 VAR).

The simulation results will allow the analysis of the behavior of DFIG magnitudes for the stator flow direction with reactive force control and rotational speed adjustment in order to maximize the active energy provided by the stator windings. For this, Matlab-Simulink was used. Figures 6 and 7 show the simulation results of the active and reactive stator forces. According to these Figures, the measured stator forces follow their active references. It is noted that this difference affects the direct rotor current, I_{rd}, and does not affect the rotor current I_{rq}, which explains why there is a separation between the active power and the I_{rd} current.

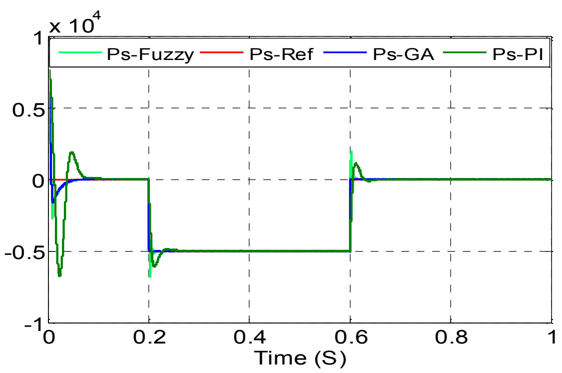

Fig. 6. Stator active power (W).

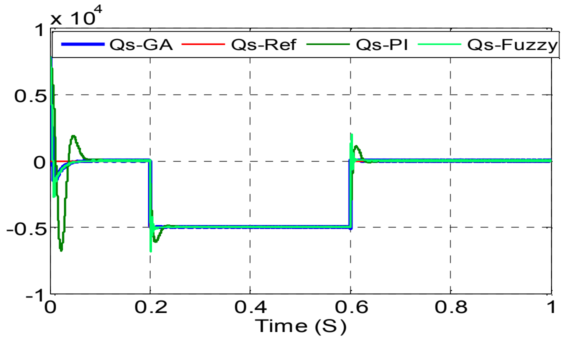

Fig. 7. Stator reactive power (VAR).

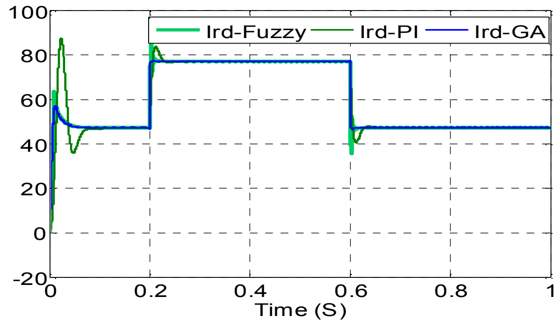

Fig. 8. The direct current of the rotor (A).

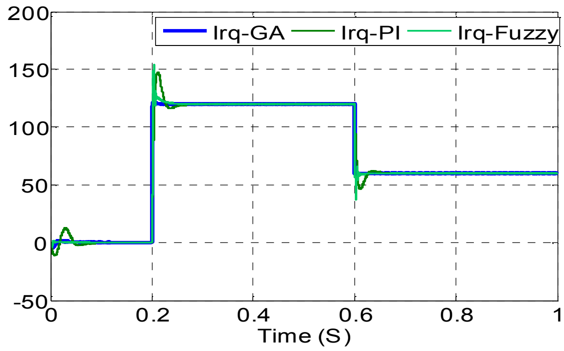

Fig. 9. The quadrature current of the rotor (A).

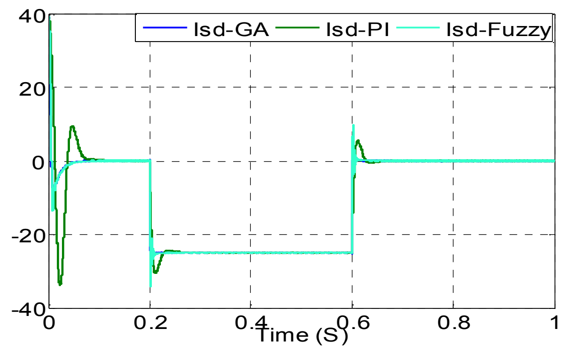

Fig. 10. The direct current of the stator (A).

Figures 8 and 9 show the simulation results of rotating currents along the d and q axes. Figures 10 and 11 show the simulation results of the stator currents along the d and q axes.

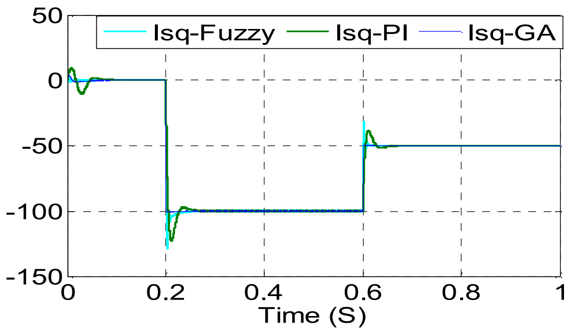

Fig. 11. The quadrature current of the stator (A).

VIII. DISCUSSION AND COMPARISON WITH OTHER WORKS

The novelty of this work is the application of GA to DFIG and its comparison with the traditional PI regulator and fuzzy logic, where in previously published works the comparison between the traditional and fuzzy regulators was made only in addition to the improvement in the obtained results. Good results were obtained compared to previously published works .

- The base table of the mysterious console was a 7×7 table, while in previously published works it was applied to a 5×5 table.
- The number of iterations increased in order to obtain more precise and better results in terms of error compared to previously published works. For a smaller number of iterations, the results were less precise. Figure 12 shows the improvement of the objective function applied to these results.

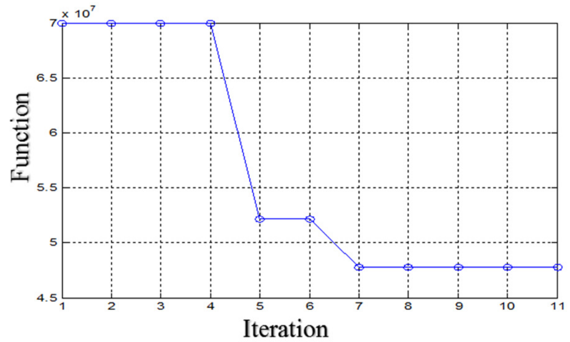

Fig. 12. Optimization of the objective function.

IX. MATLAB SIMULATION CODE

```
KP_p=kp_pmin+(kp_pmax-kp_pmin)*kp_pde/Gmax;
  KP_i=kp_imin+(kp_imax-kp_imin)*kp_ide/Gmax;
  KI_p=ki_pmin+(ki_pmax-ki_pmin)*ki_pde/Gmax;
  KI_i=ki_imin+(ki_imax-ki_imin)*ki_ide/Gmax;
%%%%%%%%%%%%%%%%%%%%%%%%%%
SELECTION AND CROSSING
%%%%%%%%%%%%%%%%%%%%%%%%%%
   [fun,index]= fate (fan);
   for i1=1:NC/2
      paron(i1,:)=POP(index(i1),:);
   end
Lu=randsrc(1,1,[1:NB-1]);
child (1:NC/4,:)=[paron(1:NC/4,1:Lu)
paron(NC/4+1:NC/2,Lu+1:NB)];
child (NC/4+1:NC/2,:)=[paron(NC/4+1:NC/2,1:Lu)
paron(1:NC/4,Lu+1:NB)];
POP=[paron ; child];
%%%%%%%%%%%%%%%%%%%%%%%%%%%
MUTATION
%%%%%%%%%%%%%%%%%%%%%%%%%%
Mu=rand(NC,NB);
   for i=1:NC
         for j=1:NB
              if Mu(i,j)<=pm
                 if POP(i,j)==1
                    POP(i,j)=0;
                 else
                    POP(i,j)=1;
                 end
              end
         end
   end
   i9=i9+1;
   fanf(i9)=Val;
end
figure
stud (funf,'-o')
title(' Function optimization objective ')
xlabel ('Itération')
ylabel('Function')
grid
```

X. CONTROL LAW

This law is a function of the error and its variation (u = f (e, Δe)). It is given by:

$$u_{k+1} = u_k + G_{\Delta u}.\Delta u_{k+1} \quad (12)$$

where $G_{\Delta u}$ is the gain associated with the order u_{k+1} and Δu_{k+1} is the variation of the order. Error e and the variation of the error Δe are normalized as follows:

$$\begin{cases} x_e = G_e.\,e \\ x_{\Delta e} = G_{\Delta e}.\Delta e \end{cases} \quad (13)$$

where G_e and $G_{\Delta e}$ are the scaling (normalization) factors. We vary these factors until we can have a transient phenomenon of suitable adjustment. Indeed, it is the latter, which will determine the performance of the command.

XI. CONCLUSION

In this paper, a fuzzy logic controller and an active and interacting GA connected to a stator network (DFIG) are considered. The fuzzy controller's effectiveness test against GA and conventional PI control under different operating conditions showed the optimum and effective performance of fuzzy controller in terms of changing rotor resistance, insensitivity to torque disturbance, low response time, accuracy, and overtaking speed, as well as faster dynamics with little error in steady state under all dynamic operating conditions. The simulation results showed good control behavior directed towards better performance of the fuzzy controller. Its superiority is particularly evident compared to the performance of the traditional control system and the GA. However, we can observe the appearance of a small error in the response of the system controlled by this type of control. The reason for this error is that the adaptation law is not fast enough to detect sudden changes in wind speed. This drawback can be limited by short sampling time. However, this choice can increase calculation time. In practice, good continuity of control allows saves energy (increases energy efficiency), increases component service life, and system performance, with more efficiency and stability.

APPENDIX

PARAMETERS OF 1.5 MW DFIG

Symbol	Parameter	Value
P_n	Rated power	1.5MW
V_s	Stator voltage	300V
F_s	Stator frequency	50Hz
R_s	Stator resistance	0.012Ω
L_s	Stator leakage inductance	0.0205H
R_r	Rotor resistance	0.021Ω
L_r	Rotor leakage inductance	0.0204H
M	Mutual inductance	0.0169H
P	Pairs of poles number	2
J	Rotor inertia	$1000Kg.m^2$

PARAMETERS OF THE TURBINE

Symbol	Parameters	Value
R	Blade radius	35.25m
N	Number of blades	3
G	Gearbox ratio	90
J	Moment of inertia	$1000Kg.m^2$
f_v	Viscous friction coefficient	$0.0024N.m.s^{-1}$
V	Nominal wind speed	16m/s
V_d	Cut-in wind speed	4m/s
V_m	Cut-out wind speed	25m/s

REFERENCES

[1] A. K. Guediri and D. Ben Attous, "Modeling and fuzzy control of a wind energy system based on double-fed asynchronous machine for supply of power to the electrical network," *International Journal of System Assurance Engineering and Management*, vol. 8, no. 1, pp. 353–360, Jan. 2017, https://doi.org/10.1007/s13198-015-0367-1.

[2] P. D. Chung, "Retaining of Frequency in Micro-grid with Wind Turbine and Diesel Generator," *Engineering, Technology & Applied Science Research*, vol. 8, no. 6, pp. 3646–3651, Dec. 2018, https://doi.org/10.48084/etasr.2413.

[3] A. Guediri and A. Guediri, "Study and Order of a Medium Power Wind Turbine Conversion Chain Connected to Medium Voltage Grid," *Engineering, Technology & Applied Science Research*, vol. 11, no. 3, pp. 7279–7282, Jun. 2021, https://doi.org/10.48084/etasr.4169.

[4] Md. R. Islam, Y. Guo, and J. G. Zhu, "Steady state characteristic simulation of DFIG for wind power system," in *International Conference on Electrical Computer Engineering (ICECE 2010)*, Dhaka, Bangladesh, Sep. 2010, pp. 151–154, https://doi.org/10.1109/ICELCE.2010.5700649.

[5] O. P. Bharti, R. K. Saket, and S. K. Nagar, "Controller Design For DFIG Driven By Variable Speed Wind Turbine Using Static Output Feedback Technique," *Engineering, Technology & Applied Science Research*, vol. 6, no. 4, pp. 1056–1061, Aug. 2016, https://doi.org/10.48084/etasr.697.

[6] R. Saini, P. Pratim Roy, and D. Prosad Dogra, "A segmental HMM based trajectory classification using genetic algorithm," *Expert Systems with Applications*, vol. 93, pp. 169–181, Mar. 2018, https://doi.org/10.1016/j.eswa.2017.10.021.

[7] A. J. P. Delima, A. M. Sison, and R. P. Medina, "A modified genetic algorithm with a new crossover mating scheme," *Indonesian Journal of Electrical Engineering and Informatics (IJEEI)*, vol. 7, no. 2, pp. 165–181, May 2019, https://doi.org/10.52549/ijeei.v7i2.1047.

[8] H. Bassi and Y. A. Mobarak, "State-Space Modeling and Performance Analysis of Variable-Speed Wind Turbine Based on a Model Predictive Control Approach," *Engineering, Technology & Applied Science Research*, vol. 7, no. 2, pp. 1436–1443, Apr. 2017, https://doi.org/10.48084/etasr.1015.

[9] I. Yaichi, A. Semmah, P. Wira, and Y. Djeriri, "Super-twisting Sliding Mode Control of a Doubly-fed Induction Generator Based on the SVM Strategy," *Periodica Polytechnica Electrical Engineering and Computer Science*, vol. 63, no. 3, pp. 178–190, Jun. 2019, https://doi.org/10.3311/PPee.13726.

[10] Z. Kara and K. Barra, "Hybrid Controller for Variable Speed Wind Energy Conversion System with Slip Energy Recovery Using Matrix Converter Topology," *Periodica Polytechnica Electrical Engineering and Computer Science*, vol. 59, no. 4, pp. 160–174, Dec. 2015, https://doi.org/10.3311/PPee.8507.

[11] S. Mondal and D. Kastha, "Improved Direct Torque and Reactive Power Control of a Matrix-Converter-Fed Grid-Connected Doubly Fed Induction Generator," *IEEE Transactions on Industrial Electronics*, vol. 62, no. 12, pp. 7590–7598, Sep. 2015, https://doi.org/10.1109/TIE.2015.2459056.

[12] W. Guo, F. Liu, D. He, J. Si, R. Harley, and S. Mei, "Reactive power control of DFIG wind farm using online supplementary learning controller based on approximate dynamic programming," in *2014 International Joint Conference on Neural Networks (IJCNN)*, Beijing, China, Jul. 2014, pp. 1453–1460, https://doi.org/10.1109/IJCNN.2014.6889871.

[13] S. A. E. M. Ardjoun and M. Abid, "Fuzzy sliding mode control applied to a doubly fed induction generator for wind turbines," *Turkish Journal of Electrical Engineering and Computer Sciences*, vol. 23, no. 6, pp. 1673–1686, Nov. 2015, https://doi.org/10.3906/elk-1404-64.

[14] J. Yang, D. Song, H. Han, P. Tong, and L. Zhou, "The integrated control of fuzzy logic and model-based approach for variable-speed wind turbine," *Turkish Journal of Electrical Engineering and Computer Sciences*, vol. 23, no. 6, pp. 1715–1734, Jan. 2015, https://doi.org/10.3906/elk-1403-295.

[15] L. Sun, Y. Chen, L. Peng, Y. Zhang, and Y. Kang, "Control winding current-oriented control for stand-alone brushless doubly fed power generation system," in *2015 IEEE Energy Conversion Congress and Exposition (ECCE)*, Montreal, Canada, Sep. 2015, pp. 2776–2781, https://doi.org/10.1109/ECCE.2015.7310049.

[16] K. Wiktorowicz, "Output Feedback Direct Adaptive Fuzzy Controller Based on Frequency-Domain Methods," *IEEE Transactions on Fuzzy Systems*, vol. 24, no. 3, pp. 622–634, Jun. 2016, https://doi.org/10.1109/TFUZZ.2015.2466111.

[17] K. Siraj, H. Siraj, and M. Nasir, "Modeling and control of a doubly fed induction generator for grid integrated wind turbine," in *2014 16th International Power Electronics and Motion Control Conference and Exposition*, Antalya, Turkey, Sep. 2014, pp. 901–906, https://doi.org/10.1109/EPEPEMC.2014.6980613.

[18] Y. Belgaid, M. Helaimi, R. Taleb, and M. B. Youcef, "Optimal tuning of PI controller using genetic algorithm for wind turbine application," *Indonesian Journal of Electrical Engineering and Computer Science*, vol. 18, no. 1, pp. 167–178, Apr. 2020, https://doi.org/10.11591/ijeecs.v18.i1.pp167-178.

[19] I. Sefa, N. Altin, S. Ozdemir, and O. Kaplan, "Fuzzy PI controlled inverter for grid interactive renewable energy systems," *IET Renewable Power Generation*, vol. 9, no. 7, pp. 729–738, 2015, https://doi.org/10.1049/iet-rpg.2014.0404.